JOURNAL OF MATERIALS SCIENCE **40** (2005) 5679–5683

Characterization of yttria-doped ceria prepared by directional crystallization

M. HARTMANOVÁ*
Institute of Physics, Slovak Academy of Sciences, 84511 Bratislava, Slovakia
E-mail: fyzihart@savba.sk

E. E. LOMONOVA
General Physics Institute, Russian Academy of Sciences, 117942 Moscow, Russia

V. NAVRÁTIL
Department of Physics, Faculty of Education, Masaryk University, 60300 Brno, Czech Republik

P. ŠUTTA
Department of Physics, Faculty of Logistics, Military Academy, 03119 Liptovský Mikuláš, Slovakia

F. KUNDRACIK
Department of Radiophysics, Faculty of Mathematics, Physics and Informatics, Comenius University, 84215 Bratislava, Slovakia

The oxygen nonstoichiometry and the related lattice defects in ceria crystals doped with the high concentration (13–26 mol%) of yttria and grown by the directional crystallization (skull technique) have been investigated. The results obtained using thermoanalysis, electrical conductivity and microhardness are described and discussed.

1. Introduction

Ceria-based materials have received an increasing attention in recent years due to their potential (unfortunately limited) of the applications as electrolyte and electrodes in the high temperature electrochemical devices, especially in the solid oxide fuel cells (SOFC) (e.g. [1]). Moreover, doped ceria is a suitable material for the fundamental studies, since it enables the low dopant compositions to be studied in order to ascertain the basic defects involved and their interactions (e.g. [2]). The addition of substitutional heterovalent ions, e.g. Y^{3+}, produces a large concentration of oxygen vacancies that is responsible for the ionic conductivity of this material.

However, these materials are known to be reduced and produce an electronic conductivity. In a fuel cell ceria-based materials are exposed to a reducing environment on the fuel side. This fact generates free electrons in the material and can lower the efficiency of energy conversion (e.g. [3]). Moreover, the high melting temperatures of ceria - based materials result in some problems at their synthesis [4]. These problems can be overcome using the skull melting technique. But the high melting temperatures and the cooling rate at this method lead very often to the oxygen nonstoichiometry. Therefore the investigation of lattice defects related to the stoichiometry changes in these materials is scientifically and technologically interesting.

From this point of view, the heavily doped ceria by yttria grown by the directional crystallization and exhibiting ionic conduction due to the formation of oxygen ion vacancies formed by doping, is the object of investigation in the present paper.

2. Experimental

2.1. Preparation of samples

The investigated crystals of $CeO_2 + y.Y_2O_3$ ($y = 0, 13, 15, 19, 26$ mol%) were prepared by the skull technique. The temperature of melting was 2770–3070 K. The growth rate of crystals was 10 mm/h. The cooling rate of grown crystals was high:

– from the temperature of crystallization down to 1270–500 K/min and
– from 1270 K down to the room temperature −40 K/min.

As—grown crystals were completely black, which indicates the oxygen nonstoichiometry, with the

* Author to whom all correspondence should be addressed.
0022–2461
DOI: 10.1007/s10853-005-2795-9

exception of CeO_2 + 15 mol% Y_2O_3 (metallic-silver colouration) and partially also CeO_2 + 13 mol% Y_2O_3. The length and the diameter of grown crystals were found to be 10–12 mm and 2–5 mm, respectively.

2.2. Lattice parameter

The unit cell parameters a of the cubic fluorite $CeO_2+y.Y_2O_3$ phases were determined by X-ray powder diffractometry using an automatic URD-6 diffractometer with the Bragg-Brentano semifocusing arrangement and CuK_α ($\lambda = 0.154178$ nm) radiation with the crystalline samples grind to powders. The lattice parameters were calculated by means of (111), (200), (220), (311) and (331) diffraction lines and the programme of M. S. Nachmanson [5].

2.3. Thermoanalytical investigation

The differential thermal (DTA) and thermo-gravimetric (TG) analyses have been performed by means of the high-temperature analyzer of Setaram (DTA 2000 K) in the temperature range of 290–1270 K in air under the following conditions: the heating and cooling rates 5 K/min, the platinum crucible, the reference material quenched Al_2O_3 powder, samples weight 100 mg.

2.4. Electrical conductivity

ac conductivity measurements were performed by an impedance technique in air. A Solartron SI 1260 impedance/gain phase analyzer interfaced to a computer and run through a Lab-view program was used. The impedance measurements were made in the frequency range 10 Hz − 1 MHz and at temperatures ∼450–820 K. The results of measurement were analysed according to the method of electrical equivalent circuit.

2.5. Vickers microhardness

Measurements were performed in air at room temperature by means of Hanneman (Vickers) microhardness tester along with a Zeiss-Neophot 32 microscope. Sample indentations were made with three loads −0.65, 0.87 and 1.1 N. The heating of samples was performed in air from the room temperature up to 670 K.

3. Results and discussion

3.1. Structural characterization

The undoped stoichiometric CeO_2 has the cubic fluorite (CaF_2) structure with the space group Fm3m over the whole temperature range from room temperature up to the melting point. The determined lattice parameter $a = 0.54105 \pm 0.00005$ nm is in a good agreement with the reported value, $a = 0.541134$ nm, e.g. [6]. The ceria structure is known to tolerate a considerable reduction without any phase change, especially at the elevated temperatures. Such CeO_{2-x} is black coloured when is nonstoichiometric.

Rare earth oxides are high soluble in ceria, about 40% or more [7]. In general, the solubilities of rare earth oxides as well as the change in the lattice parameter can be qualitatively explained by the size of cations. The ionic radii of Ce^{4+} and Y^{3+} are reported as $r_{Ce4+} = 0.0970$ nm, $r_{Ce3+} = 0.1143$ nm and $r_{Y3+} = 0.1019$ nm, respectively [8]. Additives with the ionic radii close to that of cerium cation, in our case Y^{3+}, are very soluble. A large solubility results in a great number of oxygen vacancies in the fluorite lattice. The cubic fluorite structure of the yttria-doped ceria is maintained with the slight changes in the lattice parameters depending on the composition. In agreement with the atomistic simulation calculations based on the energy minimization techniques [9], Y_2O_3—doped CeO_2 shows a negligible change in the lattice parameter also at the high defect concentrations as it can be seen in Table I.

TABLE I Lattice parameter a of CeO_2 crystals doped with high concentrations of Y_2O_3 ($y = 0 - 26$ mol%)

y (mol% Y_2O_3)	a(nm)
0	0.54105 ± 0.00005
13	0.54036 ± 0.00006
15	0.54121 ± 0.00006
19	0.54295 ± 0.00006
26	0.54234 ± 0.00006

3.2. Oxygen nonstoichiometry and related lattice defects

The high temperature of melting and the high cooling rate cause the quenching of a high-temperature state. The degree of this quenching depends on the relationship between the cooling rate and the oxygen diffusion rate (e.g. [4]). The exchange of oxygen with the atmosphere during the cooling from the temperature of crystallization is interrupted sooner than the temperature reaches its room value. This results in the oxygen nonstoichiometry, the black colour of as-grown crystals and the related lattice defects. The heating of as - grown black crystals in air, according to the thermoanalysis data, results in the oxidation process in the crystals. When the oxygen mobility (or maybe the degree of metastability) is very high, the oxidation process begins from the surface of crystal already during the process of cooling of the crystallized melt. As an example, the thermal effects taking place during the heating and registered on DTA, TG and DTG curves for undoped ceria are shown in Fig. 1. The oxidation process causes the exothermal peak at the coinciding temperature simultaneously on the DTA and DTG curves as well as the increase of weight on the TG curve. Such peaks were absent at the heating in an inert gas medium, therefore these peaks can be attributed to the oxidation process. The temperature and the rate of heating as well as the volume of the crystalline samples were chosen in such way that the oxidation process will be complete. The control of this completion was performed by the repeated heating of the same sample. When the above mentioned peak on the DTA curve was now absent and the weight of sample was maintained, it is possible to say that the oxidation process

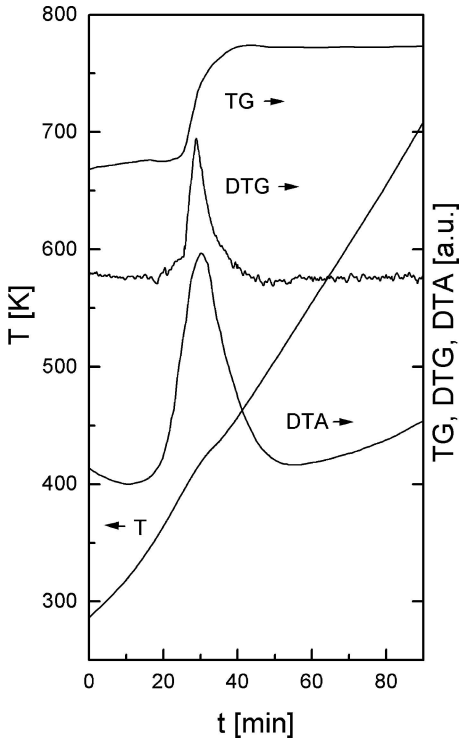

Figure 1 Thermal analysis for undoped CeO_{2-x}.

was complete and the sample reached its equilibrium state. The calculation according to the TG data allows us to estimate the degree of oxygen nonstoichiometry of the as—grown crystals (i.e. x in the $CeO_{2-x} - Y_2O_3$ formulas). The oxidation peaks were found to be extremely broad, with the width depending on the heating rate of crystal. The starting oxidation temperature was the same, 370–400 K, for all investigated crystals. The colour was changed to a metallic-silver one upon the oxidation at higher temperatures and the crystals were not transparent. CeO_{2-x} −15 mol% Y_2O_3 crystals are oxidized ($\Delta x = 0$) already at room temperature during the cooling of the crystallized melt and its decomposition into the separate single crystals. The similar behaviour was possible to observe also at CeO_{2-x} −13 mol% Y_2O_3 ($\Delta x = 0.02$) crystals. The oxidation process in the crystal doped with 15 mol% Y_2O_3 is activated by its decomposition, accompanied with the whitening (metallic-silver colouration) of crystals and their warming up to the temperatures of 330–350 K. The results obtained using the thermal analyses for all investigated crystals are shown in the Table II.

The oxygen nonstoichiometry is connected with the oxygen deficiency, which can appear at high temperatures or at low oxygen partial pressures p_{O2}. In general, the oxygen deficiency in the crystal grown in air is small. The removal of oxygen O_O^x creates the electrons e' as well as the oxygen vacancies $V_O^{\cdot\cdot}$ in the lattice via equilibrium according to the well-known Kröger-Vink notation:

$$O_O^x \leftrightarrow \frac{1}{2}O_2(g) + V_O^{\cdot\cdot} + 2e' \tag{1}$$

It means that the oxygen is exchanged with the environment and thus the oxygen must be able to diffuse through the lattice from the bulk toward the surface and *vice versa*.

The transfer of oxygen between the crystal and the atmosphere can be described by the quasi-chemical reactions [10]:

$$\begin{aligned} O_O^x &\longleftrightarrow V_O^x + \frac{1}{2}O_2(g) \quad K_1 = \left[V_O^x\right] p_{o2}^{1/2} \\ V_O^x &\longleftrightarrow V_O^{\cdot} + e' \qquad\quad K_2 = \left[V_O^{\cdot}\right][e']/\left[V_O^x\right] \\ V_O^{\cdot} &\longleftrightarrow V_O^{\cdot\cdot} + e' \qquad\quad K_3 = \left[V_O^{\cdot\cdot}\right][e']/\left[V_O^{\cdot}\right] \end{aligned} \tag{2}$$

where O_O^x is the oxygen atom in the anion site. These reactions can be used for the estimation of defect concentrations (e.g. [11]). The direct information about the density of electronic carriers and whether it is independent on the temperature for the constant degree of nonstoichiometry is possible to obtain by the simultaneous measurements of Seebeck coefficient and the electrical conductivity in the high temperature region [12].

In the case of ceria, the oxygen nonstoichiometry can be still influenced by the known property of Ce to reduce its valency state $Ce^{4+} \rightarrow Ce^{3+}$ according to the reactions [13, 14]:

$$2Ce_{Ce} + O_O^x \rightarrow 2Ce'_{Ce} + V_O^{\cdot\cdot} + \frac{1}{2}O_2(g) \tag{3}$$

or

$$Ce_{Ce} + O_O^x \rightarrow Ce'_{Ce} + V_O^{\cdot} + \frac{1}{2}O_2(g), \tag{4}$$

where $V_O^{\cdot}$ is a F-center (the electron generated by reduction and trapped at the oxygen vacancy).

TABLE II Thermoanalysis data of undoped ceria and yttria-doped ceria marerials

		Heating in air			
			DTA, TG		
Concentration of Y_2O_3 in CeO_2-Y_2O_3 crystal mol%	Colour of CeO_2-Y_2O_3 as-grown crystal	Temperature (K)	Start oxidation temperature (K)	CeO_x- Y_2O_3 (TG)	Colour of CeO_2-Y_2O_3 crystal after heating in air
0	black	1270	330	$CeO_{1.82}$	metallic-silver
13	black	1270	370	$CeO_{1.98}$-Y_2O_3	metallic-silver
15	metallic-silver	1270			
19	black	1270	400	$CeO_{1.90}$-Y_2O_3	metallic -silver
26	black	1270	400	$CeO_{1.83}$-Y_2O_3	metallic-silver

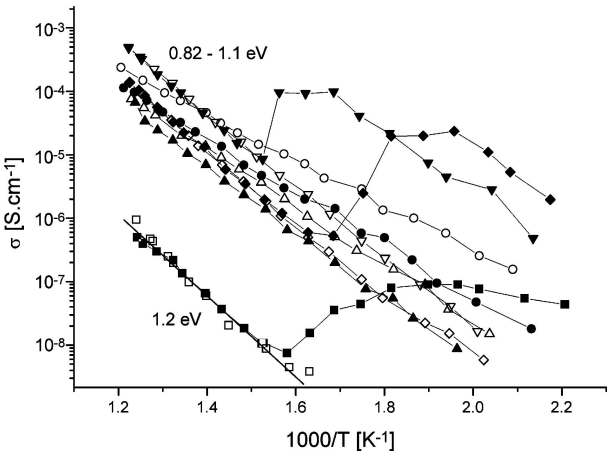

Figure 2 Arrhenius plots of electrical conductivity σ for reduced ceria single crystals doped with various amounts of Y_2O_3. As-grown crystals: (■) 0 mol%, (▲) 13 mol%, (●) 15 mol%, (▼) 19 mol% and (♦) 26 mol%; thermal-treated crystals: (□) 0 mol%, (△) 13 mol%, (○) 15 mol%, (▽) 19 mol% and (◇) 26 mol% measured in air.

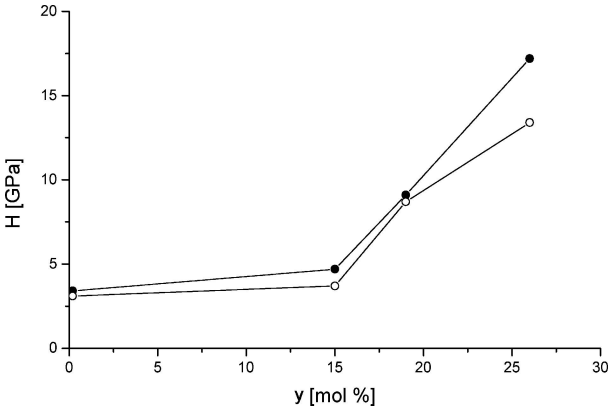

Figure 3 Microhardness H as a function of Y_2O_3 concentration y for reduced CeO_{2-x} (●) and stoichiometric (○) crystals.

3.3. Oxygen nonstoichiometry and charge transport

The electrical conductivity of undoped ceria has a mixed, *n*-type and oxygen ion, character [15]. The investigation of total electrical conductivity of undoped reduced ceria CeO_{2-x} carried out on the single crystals is presented in Fig. 2. The charge carriers in CeO_{2-x} are proposed and in general accepted (e.g. [12, 16]) to be small polarons formed by localization of electrons at cerium sites and the charge transport is proposed to occur by hopping mechanism. Whereas the ionic conductivity is always much lower than the electronic one in undoped reduced ceria, the situation is quite different in ceria doped with the oxides of two- or three-valent metals due to the introduction of oxygen vacancies.

As it is known, the doped ceria behaves as a predominantly ionic conductor under the oxidizing/low temperature conditions. The conductivity takes place by the motion of oxygen ions in the anionic sublattice. Its value is fixed by the concentration of oxygen vacancies which are created in the material when the aliovalent Y^{3+} ions are added into the CeO_2 matrix. This reaction can be written according to the Kröger-Vink notation:

$$Y_2O_3 \xrightarrow{CeO_2} 2Y'_{Ce} + 3O^x_O + V^{\cdot\cdot}_O \qquad (5)$$

The concentration of oxygen vacancies $V^{\cdot\cdot}_O$ is then dependent only on the dopant oxide content.

The conductivity behaviour for trivalent doping, in our case Y^{3+}, is attributed to the presence of $(YV_O)^{\cdot}$ pair and isolated *Y*'[2] in the low concentration range and $(Y'_2V^{\cdot\cdot}_O)$ defects with a Y-Y pair in the (100) configuration at high dopant concentration [17].

The structure of conductivity Arrhenius plots of nonstoichiometric ceria heavily doped with yttria (13, 15, 19 and 26 mol%) strongly depends on the deviation from stoichiometry, as it is possible to see in Fig. 2. The samples with the small deviation ($\Delta x = 0, 0.02$) (Table I) don't exhibit a significant change of slope over the whole investigated temperature range. On the contrary, the samples with the larger deviation ($\Delta x = 0.10, 0.07$), show a strong jog in the slope at the intermediate temperatures. The temperature of this jog varies with the composition. The thermal treatment of samples during the conductivity measurements removes these jogs (Fig. 2) probably due to the ordering of vacancies after the attainment of stoichiometry and then, the role played by the dislocations in the crystalline growth and the corresponding stress relaxation phenomena are well known (e. g. [18]). The low-temperature phase is a complex phase formed by the vacancy ordering, while the high-temperature phase is a fluorite structure with the disordered vacancies. The activation energy $E_a \sim 1.1$ eV for the crystals doped with two highest used yttria concentrations and having the higher deviations from the stoichiometry seems to be independent on the deviation from stoichiometry [19], whereas the crystals oxidized already at room temperature ($\Delta x = 0, 15$ mol%) and/or with the lower deviation from stoichiometry ($\Delta x = 0.02, 13$ mol%) have a lower activation energy, $E_a = 0.82 - 1.02$ eV.

The decrease of electrical conductivity at the highest used dopant concentration (26 mol% Y_2O_3) in the high-temperature range (Fig. 2) can be attributed to the formation of associations between the dopants and the oxygen vacancies and/or ordering of oxygen vacancies. The increase of electrical conductivity after the thermal treatment during the conductivity measurement in the case of samples with the smaller deviations from the stoichiometry ($\Delta x = 0, 0.02$) is not clear at the present.

As it was possible to see in this paper, the behaviour of reduced heavily doped ceria samples is influenced by the simultaneous effect of several factors. First of all, it strongly depends on the amount of nonstoichiometry. The deviation from stoichiometry in doped ceria arises from the formation of vacancies and possibly also from the simultaneous reduction of part of cerium ions into the trivalent state. Moreover, each of these samples has the different deviation from the stoichiometry. And then, the investigated samples contain the different concentrations of yttria. Therefore it is difficult to make any unambiguous conclusion about the influence of the separate factors.

3.4. Oxygen nonstoichiometry and microhardness

The influence of oxygen nonstoichiometry on the Vickers microhardness H was studied for the "as-grown" crystals as well as for the crystals thermally treated by the similar way as it was done during the conductivity measurements. The results obtained show that the microhardness H as a function of yttria amount increases in both investigated cases. This is in agreement with the increase of resistance against the dislocation motion in the glide plane due to the elastic interactions between the moving dislocations and the tetragonal stress field around the vacancy $-Y^{3+}$ ion complexes of various degrees or aggregates. The magnitude of this resistance depends on the kind of used impurity and on the thermal treatment of crystals [20]. It was very difficult to measure the microhardness H of investigated samples (especially the sample with 13 mol% Y_2O_3) due to the impossibility to prepare a better quality of their surface area. However, in any case, the microhardness H of reduced crystals was found to be higher compared to that of the stoichiometric ones (Fig. 3). Possible explanation of this supplementary hardness of nonstoichiometric crystalline samples might be the deformation of crystal lattice due to the removal of oxygen atoms during the melting process. The similar qualitative behaviour of microhardness H between the reduced and the stoichiometric samples was found to be also for the reduced YSZ [21].

4. Summary

The main results obtained in the investigation of the oxygen nonstoichiometry and the related lattice defects in the reduced ceria crystals doped with the high concentration of yttria and grown by the directional crystallization are as follows:

– the fluorite structure is maintained with slight changes in the lattice parameters.

– the deviation from stoichiometry Δx, the black colour of as-grown crystals and the related lattice defects arises as a consequence of the relationship between the cooling rate and the oxygen diffusion rate at the exchange of oxygen with atmosphere during the cooling from the temperature of crystallization. Heating of such reduced crystals in air results in the oxidation process in the crystals. The oxygen nonstoichiometry x in CeO_{2-x} was estimated by the thermogravimetric (TG) analysis.

– the structure of Arrhenius conductivity plots is influenced by the simultaneous effect of several factors. First of all, the strong influence of oxygen nonstoichiometry can be observed. On the contrary to the crystals with the small nonstoichiometry ($\Delta x = 0.02$), the crystals with the larger nonstoichiometry ($\Delta x = 0.07$, 0.10) exhibit a strong jog on their conductivity plots. The thermal treatment of reduced crystals during the conductivity measurements removes these jogs due to the ordering of vacancies after the attainment of stoichiometry. The investigated ceria crystals contain the different values of yttria concentration and moreover, each of crystals has different deviation from the stoichiometry. Therefore, it is difficult to make any unambiguous conclusion about the influence of separate factors.

– The microhardness H as a function of yttria amount in ceria in both the as-grown (reduced) crystals as well as in the thermal-treated (stoichiometric) ones, increases. However, the microhardness H of the reduced crystals is increased in comparison with that of the stoichiometric crystals, probably due to the deformation of crystal lattice after the removal of oxygen atoms during the melting process.

Acknowledgments

The work was partially supported by the research grant No. 2/1119/21 of the Slovak Grant Agency and FRVS MSMT 996/2000.

References

1. H. HAYASHI, M. KANOH, CHANG JI QUAN, H. INABA, S. WANG, M. DOKIYA and H. TAGAWA, *Solid State Ionics* **132** (2000) 227.
2. D. A YU WANG and A. S. NOWICK, *J. Phys. Chem. Solids* **44** (1983) 639.
3. D. S. SHINAR, D. S. TANNHAUSER and B. L. SILVER, *Solid State Ionics* **18/19** (1986) 912.
4. V. I. ALEXANDROV, V. V. OSIKO, A. M. PROCHOROV and V. M. TATARINTSEV, *Uspekhi Khimii* **47** (1978) 385.
5. M. S. NACHMANSON, software packet ANALYSIS (Compfys Laboratory-Enterprise, Saint Petersburg, Russia, 1990-1992).
6. JCPDS - International Committee for Diffraction Data, Card # 43–1002.
7. T. H. ETSELL and S. N. FLENGAS, *Chem. Rev.* **70** (1970) 339.
8. R. D. SHANNON, *Acta Crystallogr. A* **32** (1976) 751.
9. I. MINERVINI, M. O. ZACATE and R. W. GRIMMES, *Solid State Ionics* **116** (1999) 339.
10. F. A. KRÖGER, in "The Chemistry of Imperfect Crystals" (North-Holland Publ. Comp., Amsterdam, 1964).
11. M. HARTMANOVÁ, A. A. URUSOVSKAYA, M. VALKO and T. V. ORESHNIKOVA, *Solid State Phenomena* **39–40** (1994) 227.
12. H. L. TULLER and A. S. NOWICK, *J. Phys. Chem. Solids* **38** (1977) 859.
13. T. X. T. SAYLE, S. C. PARKER and C. R. A. CATLOW, *J. Chem. Soc. Chem. Commun.* **14** (1992) 977.
14. A. E. HUGHES, J. D. GORMAN, P. J. K. PATTERSON and R. CARTER, *Surf. Interface Anal.* **24** (1996) 634.
15. M. MOGENSEN, N. M. SAMMES and G. F. TOMPSETT, *Solid State Ionics* **129** (2000) 63.
16. L. K. NAIK and T. Y. TIEN, *J. Phys. Chem. Solids* **39** (1978) 311.
17. S. YAMAZUKI, T. MATSUI, T. OHASHI and Y. ARITA, *Solid State Ionics* **136–137** (2000) 913.
18. M. HARTMANOVÁ, E. E. LOMONOVA, V. NAVRÁTIL, F. KUNDRACIK and I. KOSTIC, in Proceedings of the 8th Asian Conf. "Solid State Ionics: Trends in the new millennium," edited by B. V. R. Chowdari *et al.* (World Sci. Publ. Co., Langkawi, Malaysia, Dec. 2002) p. 591.
19. M. LEVY and J. FOULETIER, *Solid State Ionics* **12** (1984) 467.
20. A. A. URUSOVSKAYA, in "Sovremennaya Kristallografyia" (Izd. "Nauka", Moscow, 1981) Vol. 4, p. 47.
21. V. R. PAI VERNEKER and D. NAGLE, *J. Mater. Sci. Lett.* **9** (1990) 192.

Received 21 May 2003
and accepted 4 April 2005